ELSEVIER

Detecting Jack Pine Budworm Defoliation Using Spectral Mixture Analysis: Separating Effects from Determinants

Volker C. Radeloff, David J. Mladenoff,* and Mark S. Boyce†*

Insect defoliation is a major disturbance force in forested ecosystems. Monitoring outbreaks, and estimating the areas affected, is therefore important for both forest managers and forest ecologists. The objective of our study was to classify jack pine budworm defoliation levels in Landsat TM imagery recorded previous to and during the 1990–1995 outbreak in our 450,000 ha study area in northwestern Wisconsin (USA). Many previous studies correlated insect defoliation and remotely sensed imagery with moderate to good success, but it often remained unclear if actual defoliation effects or other forest attributes correlated with defoliation were detected. For example, a larger deciduous component in mixed jack pine stands will limit budworm populations and thereby defoliation. The deciduous component in stands is a determining factor for insect defoliation, whereas needle discoloration and tree mortality are their effect. We used pre-outbreak Landsat TM data (1987) to identify determining factors for jack pine budworm population levels and peak-outbreak imagery (1993) for detecting actual defoliation. Our satellite data were atmospherically corrected using a radiative transfer model (5S). Spectral mixture analysis was performed using spectrometer measurements of jack pine needles and bark as representations of surface materials ("endmembers"). The explanatory power of the resulting fraction images was evaluated using jack pine budworm population data collected at 33 sampling points. Near-infrared reflectance (NIR) increased in defoliated stands between 1987 and 1993, but single date NIR in each year was negatively correlated with budworm levels in 1993 (r=−0.69 and −0.47). This was because hardwood trees within jack pine stands caused higher NIR reflectance but limited jack pine budworm populations. The 10% NIR difference between pure and mixed jack pine stands outweighed the 3–5% increase in NIR due to defoliation and necessitated stratification of the satellite data by tree species. Spectral mixture analysis performed on pure jack pine stands resulted in a strong negative correlation between the 1993 green needle fraction and the 1993 budworm population data (r=−0.94). This study was, to our knowledge, the first that applied spectral mixture analysis for forest damage detection, and also the first to use insect population measurements as independent field data. These methods, and the separation of determinants and effects of jack pine budworm defoliation, enabled us to detect actual defoliation with high accuracy.

INTRODUCTION

Insect defoliation is a major disturbance agent in forested ecosystems, a concern for resource managers, and an important area of research for ecologists. Remote sensing has been widely used to monitor insect defoliation (e.g., Nelson, 1983; Buchheim et al., 1985; Mukai et al., 1987; Hopkins et al., 1988; Leckie et al., 1989; Muchoney and Haack, 1994; Royle and Lathrop, 1997). Satellite imagery provides managers with rapid assessment of current damage so that stands with high mortality can be salvaged. It also provides scientists the opportunity to study insect defoliation over large areas so that outbreak dynamics can be related to other environmental parameters and thus be better understood and possibly forecasted (Luther et al., 1997).

* Department of Forest Ecology and Management, University of Wisconsin–Madison, Madison

† College of Natural Resources, University of Wisconsin–Stevens Point, Stevens Point

Address correspondence to V. C. Radeloff, Dept. of Forest Ecology and Management, Univ. of Wisconsin–Madison, 1630 Linden Dr., Madison, WI 53706, USA. E-mail: radeloff@facstaff.wisc.edu

Received 2 September 1998; revised 7 January 1999.

REMOTE SENS. ENVIRON. 69:156–169 (1999)

655 Avenue of the Americas, New York, NY 10010

0034-4257/99/$–see front matter
PII S0034-4257(99)00008-5

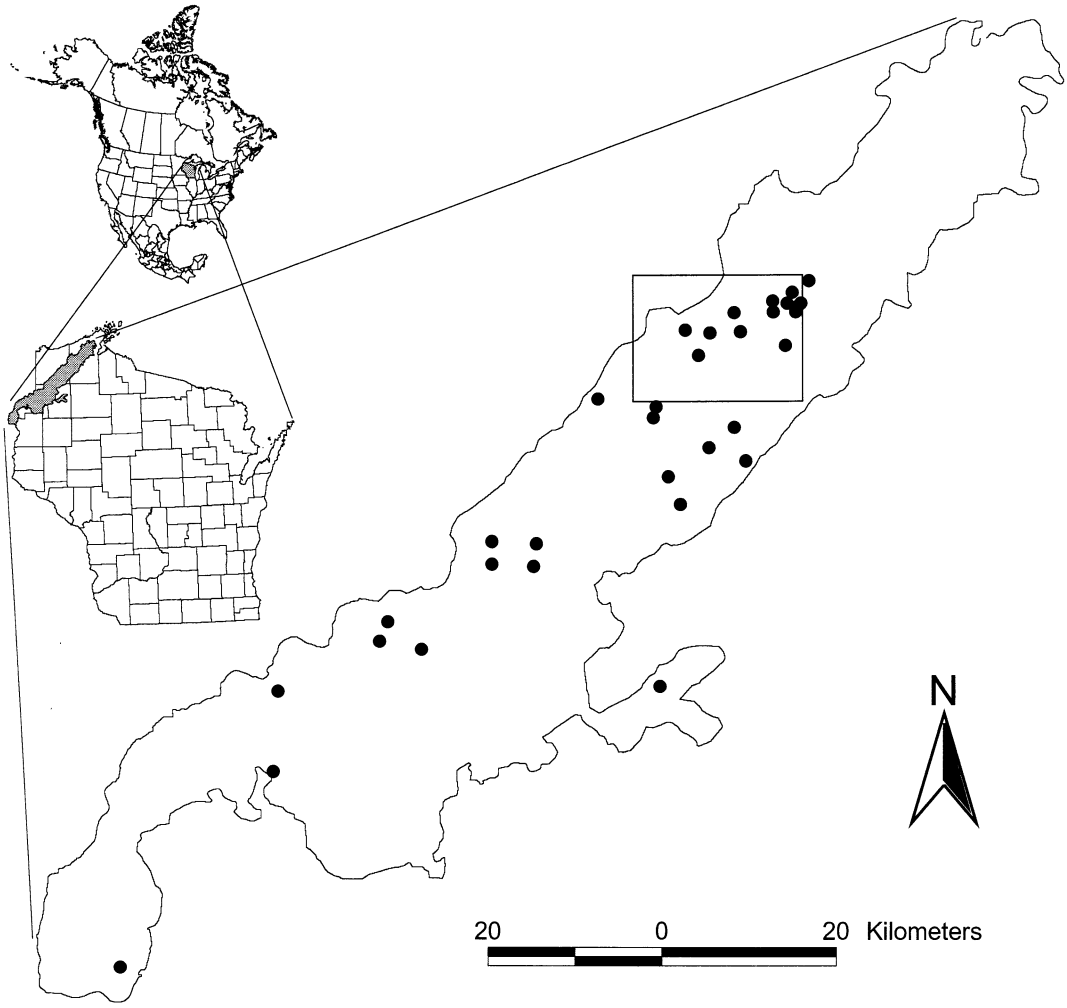

Figure 1. Location of the Pine Barrens study area in northwestern Wisconsin, USA. The 33 jack pine budworm sampling plots are shown as points. The rectangle encompasses areas of most severe defoliation examined in detail in Figure 9.

The objective of our study was to detect defoliation levels of jack pine budworm (*Choristoneura pinus pinus*) in the Pine Barrens region of northwestern Wisconsin, USA (Fig. 1). We used pre-outbreak (1987) Landsat Thematic Mapper (TM) imagery to identify forest attributes that can be remotely sensed to aid forecasting defoliation. Peak-outbreak imagery (1993) was analyzed to detect defoliation and to correlate defoliation with other ecological parameters.

The motivation for our study was twofold. First, this outbreak resulted in widespread salvage cutting of about 30% of all mature jack pine (*Pinus banksiana*) in the study area (Radeloff et al., in press) raising management concerns because of economic losses (Weber, 1995). Second, understanding natural disturbance processes is necessary for future ecosystem management of the Pine Barrens (Borgerding et al., 1995). Jack pine budworm defoliation is part of the natural disturbance regime, and our goal was to increase our scientific understanding of this ecological process.

Study Area and Jack Pine Budworm Ecology

The Pine Barrens region of northwest Wisconsin covers about 450,000 ha and is characterized by sandy soils formed on a glacial outwash plain. Fire adapted species, most notably jack pine (*Pinus banksiana*), dominated the vegetation under Native American land use before the late 19th century (Radeloff et al., 1998). Jack pine regenerates strongly after stand replacing fires due to its serotinous cones (Johnson and Gutsell, 1993). The cones remain closed until a fire melts a resin bond and releases the seeds on the open forest floor. In the absence of fire, succession may lead to oak (*Quercus* spp.) or red pine (*P. resinosa*) dominated forests. Jack pine budworm is part of the natural disturbance cycle of the Pine Barrens and appears to be well adapted to its host (Weber, 1995).

Jack pine budworm-caused mortality of jack pine increases the fuel load and thus the likelihood for a stand-replacing fire after which jack pine will regenerate more strongly than its competitors.

Defoliation levels vary spatially, and it has been suggested that defoliation is stronger on poorer sites (Weber, 1995), but the opposite was found by McCullough et al. (1996). Another possible factor is stand composition. Pure jack pine stands may exhibit higher defoliation levels than mixed stands (Weber, 1995). The same relationship has been demonstrated for spruce budworm (Su et al., 1996). The accurate detection of defoliation levels using satellite imagery would allow us to investigate these questions in the future.

Remote Sensing of Insect Defoliation

The detection of insect defoliation using remotely sensed imagery has a long history (Nelson, 1983; Buchheim et al., 1985; Williams and Nelson, 1986), and recently a study was published that employed satellite data to forecast susceptibility and vulnerability of forests to insect outbreaks (Luther et al., 1997). A special research focus has been defoliation caused by gypsy moth (*Lymantria dispar*) (Nelson, 1983; Williams and Nelson, 1986; Joria et al., 1991; Muchoney and Haack, 1994), and spruce budworm (*C. fumiferana* and *C. occidentalis*) (Ashley et al., 1976; Buchheim et al., 1985; Leckie et al., 1989; Leckie and Ostaff, 1988; Ahern et al., 1991; Leckie et al., 1992; Franklin and Raske, 1994; Franklin et al., 1995). Other studies looked at damage caused by hemlock looper (*Lambdina fiscellaria fiscellaria*) (Franklin, 1989), hemlock woolly adelgid (*Adelges tsugae*) (Royle and Lathrop, 1997), pear thrips (*Taeniothrips incosequens*) (Vogelmann and Rock, 1989), pine bark beetles (*Dendroctonus ponderosae*) (Mukai et al., 1987; Ahern, 1988; Sirois and Ahern, 1989), and tent caterpillar (*Malacosoma disstria*) (Hall et al., 1984). At least two studies examined jack pine budworm defoliation (Hopkins et al., 1988; Hall et al., 1993). Reasonably accurate satellite image classification results were obtained by classifying single images (Buchheim et al., 1985; Hopkins et al., 1988; Franklin and Raske, 1994), but change detection using multitemporal imagery has generally achieved higher classification accuracies (Mukai et al., 1987; Muchoney and Haack, 1994; Franklin et al., 1995). Insect defoliation has clearly been a major area of research in forest damage detection.

Forest Damage and Forest Change Detection

Some of the methods used for detecting insect defoliation were originally developed to detect "Waldsterben," forest damage suspected to be caused by air pollution, in remotely sensed imagery (Rock et al., 1986; Herrmann et al., 1988; Vogelmann and Rock, 1988; Westman and Price, 1988; Ekstrand, 1990; 1994). Furthermore, numerous change detection methods have been developed and applied to forests (Singh, 1989; Collins and Woodcock, 1996; Coppin and Bauer, 1996) and could be used to detect insect defoliation. Relatively robust change detection methods are image differencing (Vogelmann and Rock, 1989; Muchoney and Haack, 1994) and ratio differencing (Green et al., 1994), but they do not adequately address differences in Sun elevation angles, atmospheric conditions, or phenological changes between images recorded at different dates (Singh, 1989).

More sophisticated change detection methods perform transformations of the image space such as in Gramm–Schmidt transformation (Collins and Woodcock, 1994), principal component analysis (Fung and LeDrew, 1987; Gong, 1993), and Tasseled Cap transformation (Collins and Woodcock, 1996). Other change detection methods were based on changes in canopy cover estimates derived from a Li–Strahler canopy reflectance model (Macomber and Woodcock, 1994), and change-vector analysis (Lambin and Strahler, 1994).

Challenges in Detecting Insect Defoliation

Despite all these efforts, insect defoliation classifications have been only moderately successful. Reliable insect defoliation monitoring has often been limited to three classes (e.g., heavy, medium, and light) with accuracies around 70–80%. Low defoliation levels remain difficult to detect. Three problems make it difficult to monitor insect defoliation with satellite imagery.

First, plant–herbivore interactions are dynamic and periods where defoliation can be detected are often short. For example, hardwoods respond to defoliation by gypsy moth with a second leaf flush in late spring. This restricts the time period when defoliation can be detected to about 2 months from late June to mid-August (Williams and Nelson, 1986). Furthermore, the reflectance of defoliated trees changes over time even without direct plant responses. For example, current spruce budworm defoliation is visible as chlorosis (red discoloration) due to dead needles remaining in the canopy. Over time, these needles fall to the ground due to rain and wind, and previous defoliation is apparent as needle loss and a higher visibility of bark and branches (Leckie and Ostaff, 1988). Again, the problem is the limited time period when the most apparent change (i.e., chlorosis) can be detected (mid-July to mid-August) (Buchheim et al., 1985), because cloud-free imagery may not be available.

The second problem is that defoliation causes changes at the needle, branch, and canopy levels, and changes at one level do not necessarily translate to similar changes at others. Spectrometer measurements of *in situ* canopies are complicated to make and most measurements of damaged foliage have only been taken at the needle level (Ahern, 1988; Leckie et al., 1989). Cell structure alterations and decreasing cell water-content influence reflec-

tance change of desiccating needles, whereas canopy reflectance change is dominated by needle loss (Williams, 1991). Heavily defoliated stands might also contain stronger understory reflectance (Franklin and Raske, 1994). Another aspect of this problem is the difficulty in obtaining accurate field measurements of insect defoliation. Spectrometer measurements at the needle level are not sufficient and at the canopy level often not feasible. Visual defoliation estimates are often limited to a few defoliation classes.

The third problem is that determining factors and effects of insect population levels are both recorded in satellite imagery. For example, younger balsam fir (*Abies balsamea*) stands are more susceptible to spruce budworm defoliation than mature stands. This makes satellite-derived age maps suitable for mapping a determining factor of insect population levels useful in predicting future outbreaks (Luther et al., 1997). At the same time, the effects of insect defoliation, namely chlorosis, needle loss, and tree mortality, are apparent in satellite data (Hopkins et al., 1988; Leckie et al., 1989; 1992). When an image at the peak of an outbreak is analyzed, it is unclear if an effect (e.g., cholorosis) or a determining factor (e.g., stand age) of the insect population drives the satellite image classification. Determining factors and effects can both lead to a reasonable classification accuracy when peak-outbreak satellite imagery is analyzed. Distinguishing determining factors and effects may not be important for a forest manager mainly interested in a rapid assessment of an insect outbreak. However, separating the two, and being able to identify actual defoliation, is crucial for a scientist who may want to study, for example, the relationship between stand age and defoliation.

Given these problems, and the limited success of previous studies, we decided to employ another image transformation technique, spectral mixture analysis, to detect jack pine budworm defoliation levels during the 1990–1995 outbreak in our 450,000 ha study area in northwestern Wisconsin. Spectral mixture analysis, to our knowledge, had not previously been employed to detect insect defoliation. This technique decomposes the reflectance of each pixel into the relative contributions of a limited number of surface materials, so-called endmembers (Smith et al., 1990; Settle and Drake, 1993; Foody and Cox, 1994; Hurcom et al., 1996; Radeloff et al., 1997; Wessman et al., 1997). It has been used successfully to estimate tropical forest cover (Cross et al., 1991; Foody et al., 1997), and to measure leaf area index (LAI) and net primary production (NPP) in black spruce stands (Hall et al., 1995). Spectral mixture analysis has recently been applied to forest change detection in an area of massive deforestation in the Amazon basin (Adams et al., 1995). These studies suggested that spectral mixture analysis may be suitable to detect insect defoliation.

METHODS

Four steps comprised our satellite data processing to detect insect defoliation: a) atmospheric correction of a reference satellite scene, b) radiometric matching of two additional satellite scenes, c) separation of mixed from pure jack pine stands, and d) spectral mixture analysis using spectrometer measurements to characterize the reflectance of endmembers.

The fraction (proportion of each endmember) images resulting from the spectral mixture analysis of images recorded at the peak of the outbreak (1993) were correlated with population measurements of jack pine budworm at 33 sampling locations from the same year. We also correlated 1993 budworm population data with 1987 satellite data.

Atmospheric Correction Using 5S

Our decision to use spectrometer measurements as representations of possible surface materials made it necessary to correct the satellite imagery for atmospheric effects. We performed an atmospheric correction using a radiative transfer model on the Landsat TM scene recorded at the peak of the outbreak (1 August 1993). This scene was also the one with the least visible atmospheric disturbance in the three optical bands.

The 5S (Simulation of the Satellite Signal in the Solar Spectrum) model version used in our study was developed by Tanré et al. (1979; 1985) and modified by Hill (1993; Hill et al., 1995) to include pixel adjacency effects (Tanré et al., 1987). Topographic effects are not taken into account, an assumption valid in our study area because of the lack of steep terrain (Proy et al., 1989; Radeloff et al., 1997).

The most crucial step in the atmospheric correction is to estimate the aerosol optical thickness at the time a satellite scene was recorded. The aerosol optical thickness τ_a can be approximated for a given wavelength λ using Eq. (1):

$$\tau_a = b \cdot \lambda^{-n} \quad (1)$$

The 5S model derives the parameters b and n, the so-called Ångstrom parameters, that are related to the concentration of aerosol optical particles. These parameters are derived from the comparison of a spectral signature of a water body in the satellite image with a water reference signature measured with a spectrometer. No spectrometer measurements of water bodies in or near our study area were available. We tested two signatures ("clear" and "very clear") measured by Dekker and Donze (1994) that are incorporated in the version 5S program employed in this study. Additionally, we used three reflectance measurements (site 23: 14 August 1983; site 28: 12 and 14 August 1983) taken by Hall et al. (1992) from helicopters over lakes in the Superior National Forest, Minnesota (Fig. 2). From the satellite im-

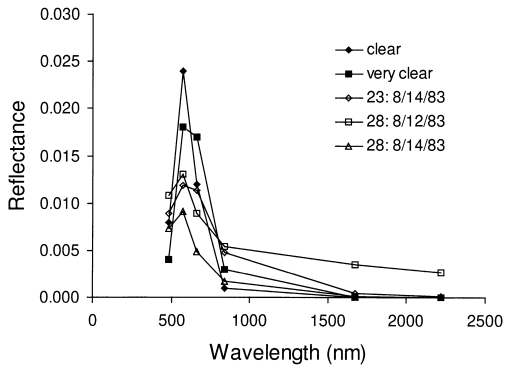

Figure 2. Spectrometer measurements of lakes tested for parametrizing the atmospheric correction.

agery, we selected eight lakes and derived Ångstrom parameters, atmospheric thickness, and the correlation factor (Hill, 1993) for 40 possible combinations between satellite and ground measurements. Out of these, we selected the optimal combination based on the correlation factor and the Ångstrom parameters. A sensitivity analysis was performed using reflectances resulting from several combinations of b and n. Furthermore, we compared jack pine canopy reflectance in the satellite scene with measurements taken from helicopters during the BOREAS (Boreal Ecosystem Atmosphere Study) field campaign in Canada (C. Walthall, individual and unpublished data).

Radiometric Matching

Two additional satellite scenes (14 June 1987; 10 May 1992) were radiometrically matched to the atmospherically corrected scene (Coppin and Bauer, 1994). We selected signatures from pseudo-invariant image objects to derive regression lines. Suitable areas included lakes, airport runways, railyards, and polygons over the urban center of Duluth, Minnesota. These dense urban areas are not homogeneous, but they contain very limited amounts of vegetation and exhibit little change over time. The accuracy of the radiometric matching was evaluated using a second set of independent pseudo-invariant image objects and by comparing coniferous vegetation reflectance between the two summer scenes.

Budworm Population Field Data and Satellite Data Correlations

The budworm population field data were collected by entomologists from the Wisconsin Department of Natural Resources (WDNR, R. Endreson, unpublished data). The number of early jack pine budworm larvae were measured in late spring on 30 shoots on each of 33 randomly located plots. We visually defined polygons of homogeneous jack pine stands surrounding the budworm sampling plots in the satellite imagery and measured reflectance values in the satellite imagery previous to the outbreak (1987) and at the peak of the outbreak (1993). These reflectance values and the difference between the two dates were then correlated with the budworm population data.

The correlation of the 1993 budworm data with the 1993 satellite data and with the difference between 1993 and 1987 addressed our first goal of detecting current defoliation. Our second goal, to examine the potential of pre-outbreak satellite data to predict later budworm populations, was addressed by correlating the 1993 budworm data with the 1987 satellite data.

Separation of Mixed and Pure Jack Pine Stands

Phenological changes between our spring (May) and summer (June) imagery were utilized to reveal stands with varying proportions of hardwood canopy. The increase of near-infrared reflectance (NIR) between these two dates was significantly higher where hardwood was present. An analysis of our 33 budworm population sampling points allowed the determination of a threshold of NIR increase above which we assumed that a pixel contained hardwood and had to be excluded from the analysis.

This threshold and the species-level forest classification by Wolter et al. (1995) allowed us to create a mask of pure jack pine that was applied to all three satellite images. Forest clear-cuts that occurred between 1987 and 1993 were eliminated from the change detection analysis. A previous study identified clear-cuts based on their higher reflectance in TM5 (Radeloff et al., in press).

Spectral Mixture Analysis

The spectral mixture analysis of the satellite data was based on a linear demixing algorithm that involves the simultaneous solution (using least squares) of two equations of the form shown in Eq. (2):

$$\rho_b = \sum_{i=1}^{N} F_i \cdot \rho_{i,b} + E_b \qquad \text{and} \qquad \sum_{i=1}^{N} F_i = 1 \qquad (2)$$

The solution minimizes the errors E over all bands b where ρ_b is reflectance in the satellite image in band b, $\rho_{i,b}$ is the reflectance of endmember i in band b, F_i is the fraction of endmember i, and N is the number of endmembers (Smith et al., 1990). The error E gives an estimate of the fit of a given endmember set when applied to the satellite data.

We collected 11 spectrometer measurements of four different types of vegetative material (jack pine bark, dry jack pine needle, green jack pine needle, and aspen leaf), and used their reflectance values in the Thematic Mapper bands as input for the spectral mixture analysis (Fig. 3). The measurements came from two sources. An extensive NASA study in the Superior National Forest (Hall et al., 1992) provided spectra for jack pine bark (Sample PB0B201R: bark 5), jack pine needle upper surface (PB0N2T1R, PBLR: green needles 1 and 2), and aspen leaf upper surface (A25H29RF, A25M11RF, leaves

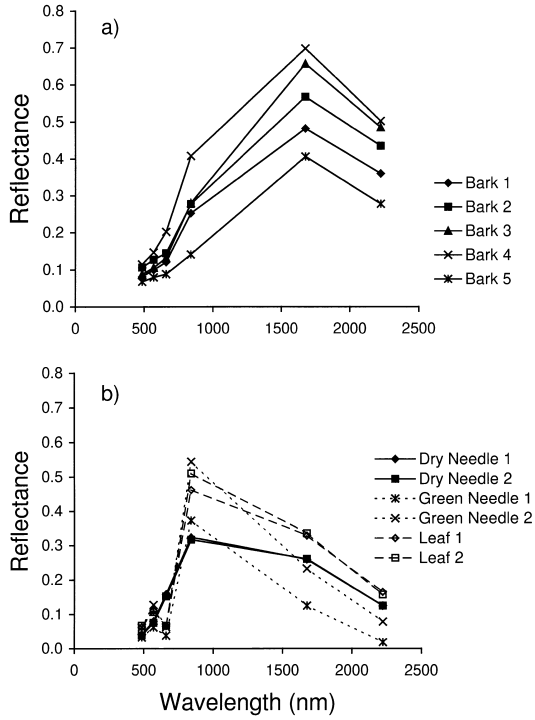

Figure 3. Spectrometer measurements used to characterize the endmembers for the spectral mixture analysis: (a) jack pine bark and (b) dry jack pine needles, green jack pine needles, and green aspen leaves.

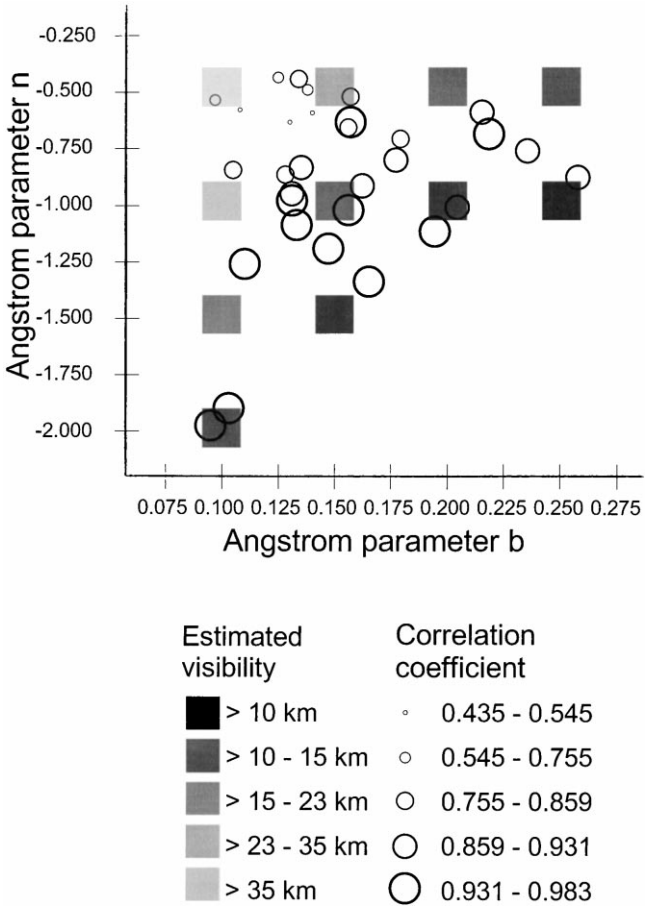

Figure 4. Correlation factors for lake/reference spectra pairs (circles) and estimated visibility (boxes) for different combination of the Ångstrom parameters b (x-axis) and n (y-axis).

1 and 2), that were aggregated to the wavebands of Landsat TM (Hall et al., 1992). We measured additional spectra of dry jack pine needles (dry needles 1 and 2) and jack pine bark (barks 1–4) using an ASD (Analytical Spectral Devices) Spectroradiometer with a range of 350-2500 nm. A shade endmember was included assuming zero reflectance in all channels. The limited dimensionality of Landsat TM images does not allow reliable use of more than three or four endmembers. We tested numerous endmember sets and evaluated them in relationship to our budworm population field data. The endmember set that exhibited the highest correlation with the jack pine budworm population data was used to perform spectral mixture analysis of the satellite data of all pure jack pine stands.

RESULTS

Satellite Data Preprocessing

The atmospheric correction required choosing a set of two water signatures; one measured in the satellite image and one measured by a spectrometer. Different combinations of five reference spectra and eight lake spectra resulted in different estimations of the Ångstrom parameters b and n, correlation factors, and estimated visibilities (Fig. 4). We chose the combination with the highest correlation factor ($r=-0.983$) and average Ångstrom parameters $b=0.156$, $n=-1.039$. The atmospheric correction appeared to be robust with respect to different combinations. Very different pairs of Ångstrom parameters with almost equally high correlation factors resulted in

Figure 5. Reflectance of two coniferous stands after atmospheric corrections with different pairs of Ångstrom parameters.

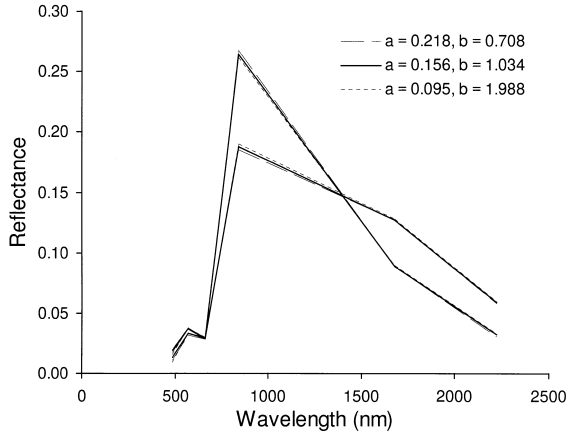

Table 1. Regression Factors for the Radiometric Matching between the Atmospherically Corrected Imagery (August 1993) and the Two Other Satellite Images[a]

	Jun-87			*May-92*		
	r^2	*Mean Error*	*Maximum Error*	r^2	*Mean Error*	*Maximum Error*
TM1	0.9876	0.0067	0.0200	0.9905	0.0032	0.0059
TM2	0.9929	0.0057	0.0168	0.9944	0.0030	0.0058
TM3	0.9942	0.0062	0.0169	0.9920	0.0076	0.0141
TM4	0.9929	0.0079	0.0153	0.9907	0.0063	0.0148
TM5	0.9976	0.0056	0.0107	0.9939	0.0053	0.0119
TM7	0.9975	0.0047	0.0103	0.9962	0.0035	0.0079

[a] Errors measured at independent control areas are given in reflectance scaled from 0 to 1.

similar estimates for the aerosol optical thickness. Accordingly, signatures of forest stands in the corrected satellite imagery always showed less than 1% difference in reflectance when extremely different Ångstrom parameters were tested (Fig. 5). Relative differences were highest in TM Band 1, the blue band, where atmospheric effects are strongest, and in TM Band 4, the near-infrared reflectance band in which vegetation exhibits the highest absolute reflectance values.

The radiometric matching resulted in strong correlations between the atmospherically corrected satellite image and the two other scenes (Table 1). Average errors were always lower than 1% reflectance for all bands.

Reflectance of six nondefoliated jack pine stands in the northernmost portion of the Pine Barrens was measured in the satellite imagery from 1987 and 1993 (Fig. 4). No systematic changes occurred between these two dates. Furthermore, the signatures correspond well with spectrometer measurements of jack pine canopies taken during the BOREAS project from helicopters that were close enough to the ground to be free of atmospheric effects (Fig. 6).

Figure 6. Reflectance of six nondefoliated jack pine stands in the atmospherically corrected (1993) and radiometrically matched (1987) satellite data, plus reflectance of three jack pine stands measured with a spectrometer mounted on a helicopter during the BOREAS field campaign.

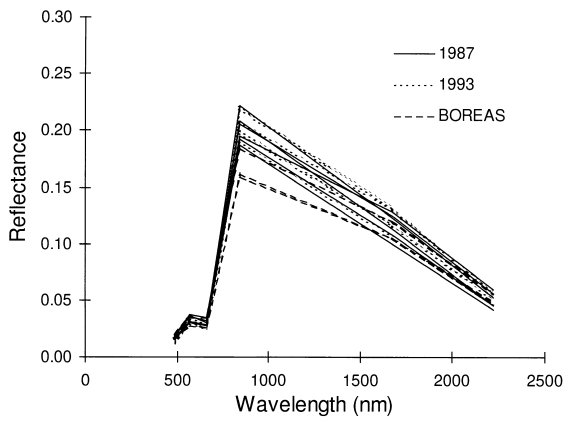

Reflectance Changes Due to Defoliation

The transformation of the satellite data into reflectance allowed us to quantify changes caused by jack pine budworm defoliation. We selected six stands that were heavily defoliated in 1993 and extracted their reflectance from the 1987 and 1993 imagery (Fig. 7). These defoliated stands exhibited a reflectance increase in the near- and mid-infrared wavelength. The strongest change occurred in TM Band 4 with a maximum of 8% reflectance increase (5% average).

This NIR increase seems to be contradicted by the negative correlation ($r=-0.47$) between the 1993 budworm population data and the 1993 satellite data (Fig. 8a). The negative correlation was even stronger between 1993 budworm populations and 1987 satellite data ($r=-0.69$; Fig. 8b). Correlograms with 95% confidence intervals showed no significant autocorrelation in the 1993 budworm data and the 1987 and 1993 NIR. The stratification of the 33 sampling locations into mixed and pure jack pine stands (Fig. 8) revealed that highest NIR oc-

Figure 7. Reflectance of six heavily defoliated jack pine stands in the atmospherically corrected (1993) and radiometrically matched (1987) satellite data.

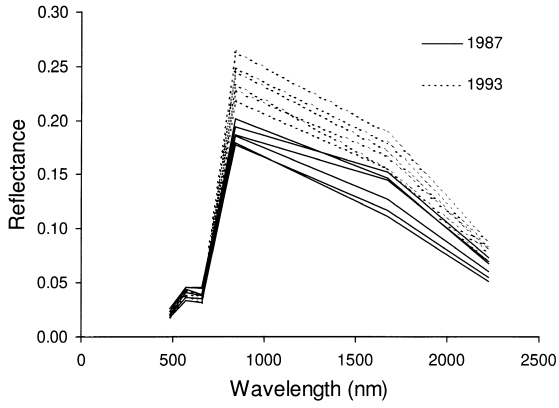

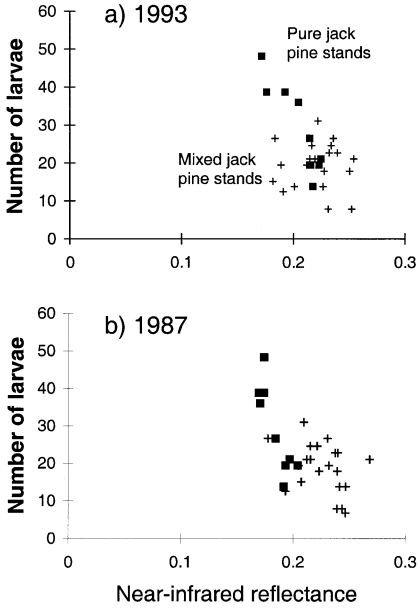

Figure 8. Relationship between budworm population levels recorded at the peak of the outbreak (1993) and NIR reflectance of forest surrounding the sampling plots measured in the imagery of a) 1993 and b) 1987. (■: pure jack pine stands; +: mixed jack pine stands).

curs in mixed stands with low budworm population levels. The NIR increase at our sampling points between 1987 and 1993 (max 3.5%) was overruled by the ~11% NIR range (max=28%, min=17%) exhibited by all pure and mixed jack pine stands in 1987. The NIR increase between 1987 and 1993 was positively correlated with the budworm population levels, but the correlation was weak (r=0.48).

Separation of Mixed and Pure Jack Pine Stands

The effect of hardwood components on the reflectance measurements made it necessary to separate mixed from pure jack pine stands. The forests surrounding our 33 budworm sampling points were used as calibration data. We examined NIR in a spring (May 1992) and a summer (June 1987) scene. Hardwoods flushed between these two dates resulting in a strong increase in NIR of mixed jack pine stands between the two images (mean NIR increase: 5.1%; standard deviation: 2.1%). Pure jack pine stands did not exhibit similar changes (mean NIR increase: 1.6%; standard deviation: 1.3%). The NIR increase of mixed and pure stands was significantly different (df=15, p<0.005) and we employed a 3% NIR increase threshold above which a pixel was assumed to contain a significant hardwood component. Using this threshold, 26% of the area classified by Wolter et al. (1995) as jack pine was eliminated from further analysis due to hardwood mixture.

Spectral Mixture Analysis

Comparisons of various three- and four-endmember models to the 1987 and 1993 imagery revealed that three-endmember models always achieved a better fit and better correlation with the budworm population data. Therefore, only results for the three-endmember model will be presented. We limited endmember combinations to ecologically meaningful sets. These always included one shade endmember, one endmember representing nonphotosynthetic vegetation (NPV; bark or dry needle), and one endmember representing green vegetation (green needle or leaf), resulting in 28 possible combinations.

The aspen leaf endmembers were included to test if hardwood content could be separated, thus avoiding the intermediate step of separating pure and mixed jack pine. This test was not successful. Endmember sets with aspen leaves representing green vegetation resulted in negative fractions for the NPV endmember, and correlations with the budworm data were always weaker compared to endmember sets with green needle endmembers.

The comparison of average fractions calculated from the reflectance values of the 10 pure jack pine stands surrounding budworm sampling points showed highly variable results for different endmember sets (Table 2). For example, the average NPV endmember fraction in the 1993 scene varied from 0.110 (bark 4, green needle 1) to 0.338 (dry needle 2, green needle 1). Despite this variability, there were some general trends. For each endmember set, the shade fraction decreases from 1987 to 1993 (average decrease of all endmember sets: 0.043), the green needle fraction increases (average: 0.035), as does the bark fraction somewhat (average: 0.008). Endmember sets with a dry needle endmember always resulted in a higher NPV fraction than sets with bark endmembers.

One criterion for the selection of endmember sets was their fit (i.e., the errors associated with them). Endmember sets with a dry needle spectrum consistently resulted in higher errors than endmember sets with a bark spectrum. Green needle 1 resulted in lower errors than green needle 2 when combined with any bark spectrum.

Our second criterion was the explanatory power of the resulting fractions when correlated with the 1993 budworm data (Table 3). All endmember sets containing a bark spectra exhibited strong correlation factors (r~−0.94) for their green vegetation spectrum. Endmember sets with dry needle spectra exhibited lower correlation factors than those with bark spectra.

Correlation factors for the 1993 satellite imagery were always higher than for the 1987 imagery. Fraction differences between the two images had low correlation factors. Within the endmember sets with bark spectra, green needle 1 was better suited for the 1987 image, and green needle 2 for the 1993 image. We chose the end-

Table 2. Resulting Fractions and Errors of Spectral Mixture Analyses with Various 3-Endmember Sets Always Containing a Shade, a Nonphotosynthetic Vegetation (NPV), and a Green Vegetation Endmember[a]

		Fractions							
		Pre-Outbreak (1987)			*Peak-Outbreak (1993)*			*Errors*	
NPV Endmember	*Green Veg. Endmember*	*NPV*	*Green Veg.*	*Shade*	*NPV*	*Green Veg.*	*Shade*	*1987*	*1993*
Bark 1	Green needle 1	0.144	0.406	0.450	0.156	0.445	0.399	0.005	0.007
	Green needle 2	0.104	0.293	0.602	0.112	0.321	0.566	0.007	0.010
Bark 2	Green needle 1	0.119	0.415	0.466	0.128	0.455	0.417	0.005	0.008
	Green needle 2	0.085	0.299	0.617	0.091	0.327	0.582	0.008	0.011
Bark 3	Green needle 1	0.105	0.425	0.470	0.114	0.465	0.421	0.004	0.006
	Green needle 2	0.075	0.303	0.622	0.082	0.331	0.587	0.007	0.009
Bark 4	Green needle 1	0.102	0.391	0.507	0.110	0.429	0.461	0.004	0.008
	Green needle 2	0.120	0.309	0.571	0.129	0.338	0.533	0.008	0.010
Bark 5	Green needle 1	0.169	0.437	0.394	0.183	0.478	0.339	0.005	0.008
	Green needle 2	0.120	0.309	0.571	0.129	0.338	0.533	0.008	0.010
Dry needle 1	Green needle 1	0.320	0.228	0.452	0.331	0.269	0.400	0.012	0.017
	Green needle 2	0.255	0.196	0.549	0.252	0.232	0.516	0.011	0.015
Dry Needle 2	Green Needle 1	0.326	0.228	0.446	0.338	0.268	0.394	0.012	0.016
	Green needle 2	0.262	0.194	0.544	0.261	0.229	0.510	0.010	0.014

[a] The spectral analysis was conducted over 10 pure jack pine stands surrounding jack pine budworm sampling plots.

member set with bark 2, green needle 2, and shade as the final set for the spectral mixture analysis of the 1993 satellite image (Fig. 9). This endmember set exhibited a good fit, a relatively high correlation for the 1993 NPV fraction, and the highest correlation factor for the 1993 vegetation fraction.

DISCUSSION

Satellite Data Preprocessing

The satellite data preprocessing, atmospheric correction, and radiometric matching performed reliably as demonstrated by the results of our sensitivity analyses (Figs. 5 and 6). The good correspondence among jack pine signatures in the corrected satellite imagery, and as measured during the BOREAS field campaign, indicated that the atmospheric correction of the satellite data indeed removed atmospheric effects. The only systematic difference was a lower NIR for the BOREAS measurement that could potentially be due to the lower leaf area index of the Canadian jack pine stands compared to those in northwestern Wisconsin.

A possible source of error in the atmospheric correction process was the choice of a reference target lake and a reference water spectrum to estimate atmospheric thickness in the 5S model. Some combinations exhibited low correlation factors. The reason for this is that the water of a given lake and a reference spectrum may have different properties (e.g., turbidity, nutrient content). The literature contains few spectrometer measurements over lakes and further research in this area would be valuable (Dekker and Donze, 1994). However, it is encour-

Table 3. Correlation Coefficients (r) of Different Fractions with the 1993 Budworm Population Data at 10 Sampling Points in Pure Jack Pine Stands

		Pre-Outbreak (1987)			*Peak-Outbreak (1993)*				*Fraction Differences (1987–1993)*	
NPV Endmember	*Green Veg. Endmember*	*NPV*	*Green Veg.*	*Shade*	*NPV*	*Green Veg.*	*Shade*	*NPV*	*Green Veg.*	*Shade*
Bark 1	Green needle 1	−0.345	−0.745	0.767	0.292	−0.943	0.790	0.440	−0.598	0.570
	Green needle 2	−0.215	−0.748	0.727	0.420	−0.941	0.599	0.469	−0.597	0.758
Bark 2	Green needle 1	−0.338	−0.754	0.772	0.299	−0.941	0.821	0.442	−0.591	0.633
	Green needle 2	−0.216	−0.751	0.741	0.417	−0.943	0.676	0.465	−0.606	0.768
Bark 3	Green needle 1	−0.350	−0.761	0.773	0.283	−0.941	0.828	0.434	−0.582	0.184
	Green needle 2	−0.233	−0.765	0.751	0.407	−0.938	0.706	0.467	−0.577	0.727
Bark 4	Green needle 1	−0.339	−0.736	0.780	0.289	−0.942	0.886	0.437	−0.608	0.699
	Green needle 2	−0.216	−0.766	0.684	0.420	−0.936	0.430	0.469	−0.573	0.746
Bark 5	Green needle 1	−0.342	−0.769	0.742	0.295	−0.937	0.668	0.443	−0.571	0.549
	Green needle 2	−0.216	−0.766	0.684	0.420	−0.936	0.430	0.469	−0.573	0.746
Dry needle 1	Green needle 1	−0.280	−0.464	0.770	0.341	−0.832	0.794	0.445	−0.572	0.749
	Green needle 2	−0.163	−0.514	0.637	0.455	−0.850	0.322	0.470	−0.572	0.712
Dry needle 2	Green needle 1	−0.286	−0.465	0.765	0.338	−0.832	0.782	0.446	−0.575	0.772
	Green needle 2	−0.174	−0.510	0.632	0.446	−0.849	0.311	0.467	−0.577	0.752

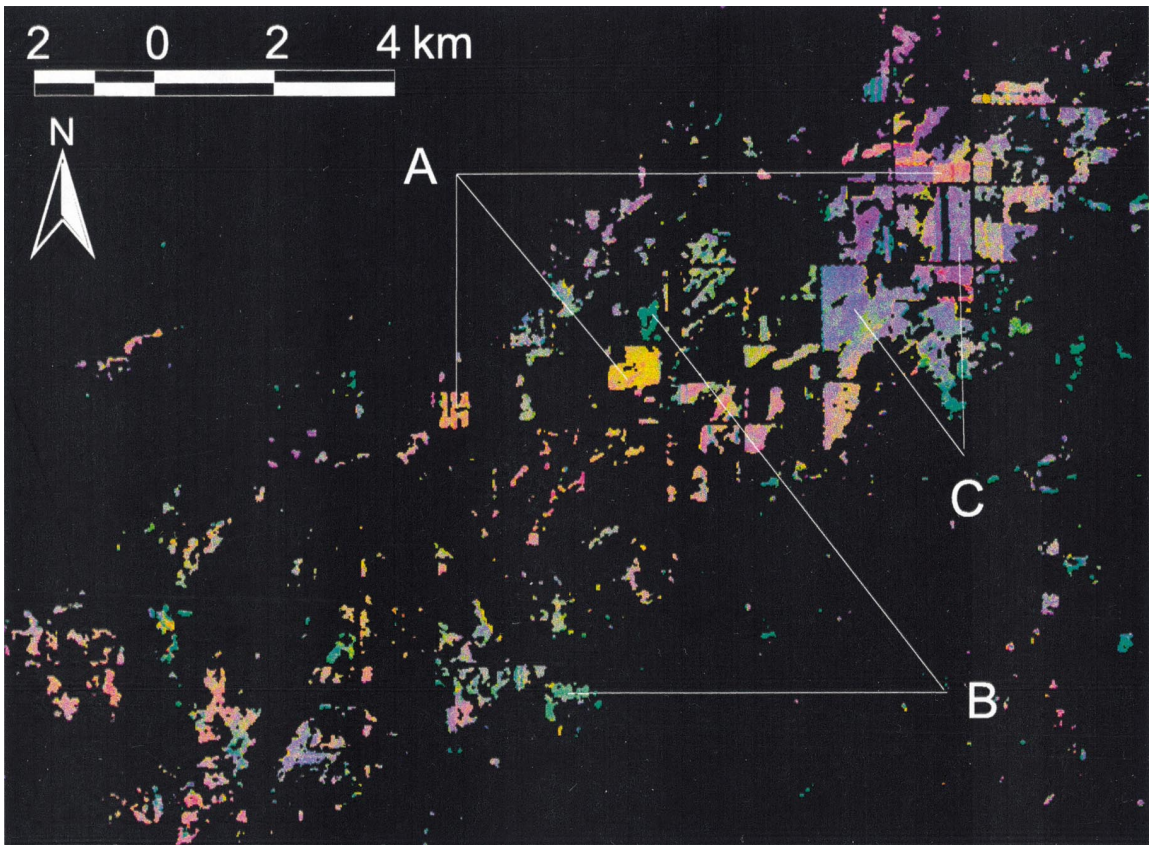

Figure 9. Color-composite of the images fractions (red: bark, green: green vegetation, blue: shade) for pure jack pine stands in the central part of the Pine Barrens, where defoliation levels were highest (compare Fig. 1 for the location of the map within our study area). Red and yellow areas (A) exhibited highest defoliation, characterized by a high bark and low green needle fraction, and were subsequently salvaged cut. The green areas (B) contain the highest vegetation fractions. These stands were classified as jack pine by Wolter et al. (1995), and thus included in our analysis, but field checking revealed that they had been falsely classified red pine. Red pine was not defoliated and the spectral mixture analysis did distinguish these stands by calculating a very high green needle fraction. The blue areas (C) are characterized by strong shade fractions. Defoliation in these areas was lower, and these stands survived the outbreak.

aging that the results of the atmospheric correction were robust in terms of the choice of input parameters such as water spectrometer measurements and target lakes in the imagery.

The reliability of the radiometric matching was indicated by the magnitude of the correlation factors in the regression equations, and the low variability measured over independent pseudo-invariant targets (Table 1). Highest variability occurred in the case of signatures taken over urban centers. These signatures were nevertheless used to establish the regression equations because they provided midrange values. Without them, the regression would have only been based on two types of targets, dark lakes and extremely bright surfaces, such as runways, possibly inflating correlation coefficients artificially.

NIR Increase with Defoliation

One surprising result of our study was the NIR increase after jack pine stands were defoliated. Studies of other conifers and deciduous species showed a decrease of NIR in response to insect outbreaks (Ahern, 1988; Leckie et al., 1989). Decreasing NIR was also observed in the case of other conifers damaged by air pollution (Vogelman and Rock, 1988). However, NIR increase after defoliation was previously reported in a study of damaged pine in Germany (Herrmann et al., 1988). Jack pine needles damaged due to porcupine girdling showed higher reflectance at wavelengths >830 (nm), as did eastern white pine (*P. strobus*) needles damaged by herbicide spraying at >840 (nm) (Leckie et al., 1989). The underlying physiological reasons for this NIR increase in different pine species are not understood. Defoliation in pine causes reflectance changes that differ from those in other conifers such as spruce and fir. This may be the result of differences in crown architecture or stand structure, or both. It has been suggested that the NIR increase of pine at the canopy level might be due to chlorosis (the retention of dead needles in the crown;

Herrmann et al., 1988). Another possible factor could be an increasing contribution of the forest understory to the reflectance measured in defoliated stands (Häne 1991). Pine forest canopies are often more open than spruce or fir forest canopies. We were not able to conduct understory measurements because all defoliated stands were salvaged, and therefore the NIR increase cannot be explained at this point.

Even though the underlying reasons for the NIR change are not understood, the increase has been repeatedly documented for defoliated pine. This suggests that common vegetation indices may not be suitable for studies of forest damage in pine forests. Indeed, preliminary tests with our data showed higher NDVI values after defoliation and no significant correlation between NDVI and budworm population data. Similarly, higher degrees of pine-needle discoloration due to air pollution in the St. Petersburg region resulted also in higher NDVI values (Donchenko et al., 1998).

Spectral Mixture Analysis

Spectral mixture analysis transformed the image space so that the resulting fraction images correlated well with the budworm population field data. This is encouraging because the field data exhibited a wide range of budworm population levels at the peak of the outbreak (Fig. 8). However, the estimated fractions were quite variable for different endmember sets (Table 2). Our resulting fractions cannot be interpreted as the percentage of dead needles or the percentage of trees being defoliated. The spectral mixture analysis provided a transformation of the satellite data feature-space specific to our research question. Unlike principal component analysis, the use of endmembers allowed the transformation of the satellite data into fraction images related to ecologically meaningful components of surface materials. Spectral mixture analysis resulted in high correlation factors between our fraction images and budworm population data (Table 3). These high correlations are the ultimate test of our approach. Each step of our satellite data analysis (atmospheric correction, radiometric matching, and spectral mixture analysis) introduced potential errors. The high correlation achieved by the final product makes it suitable for studying jack pine budworm defoliation. The RGB color composite of the three fraction images detected defoliation well (Fig. 9).

The algorithm used for the spectral mixture analysis assumed a linear relationship between surface materials and the relative contribution of endmember signatures to satellite-measured reflectance. This assumption is problematic for vegetation, because of radiation transmitted through leaves and reflected by other surface materials. This radiation exhibits a green peak and will inflate the green component in the spectral mixture analysis (Roberts, 1993; Borel and Gerstel, 1994). We chose not to use a nonlinear algorithm. The noise inherent in Landsat TM measurements most likely overrules nonlinear mixture effects (Adams et al., 1995). Transmission is 50% lower for needles compared to leaves thus reducing nonlinear effects in conifers (Hall et al., 1992). Furthermore, it was not our goal to derive absolute surface fractions, but rather to transform the satellite data so defoliation could be detected more reliably.

Three Problems for the Remote Detection of Insect Defoliation

We outlined above three major problems that complicate satellite data analysis of insect defoliation: a) short time windows for detection, b) different responses at needle, branch, and canopy scales, and c) the separation of determining factors for, and effects of, higher insect population levels. Our study of jack pine budworm defoliation addressed all three of these problems.

Jack pine budworm defoliation was most apparent in the second half of July as chlorosis, but cloud-free imagery close to this date was only available for one year (1993) during the six years of the outbreak (1990–1995). Preliminary analysis of other satellite scenes (April 1991, May 1992, May 1995) indicated that phenological differences between spring and summer scenes were stronger than reflectance changes due to defoliation. Tracing defoliation annually was not possible due to the lack of cloud-free imagery recorded at the time when defoliation effects were strongest.

The spectrometer measurements of jack pine needles available to us showed lower NIR for dry versus green needles. However, NIR of jack pine stands increased with defoliation and this increase was positively correlated to jack pine budworm population levels. It is not understood why this increase occurs and why pines exhibit the opposite reflectance change after defoliation than spruce or deciduous stands. Spectral mixture analysis offers a quantitative framework for using needle-level spectrometer measurements as input for the analysis of canopy-level satellite measurements. However, spectral libraries contain only few measurements of healthy and desiccating vegetation. More research focused on reflectance changes over time, and on the underlying physiological causes, is needed.

Determining factors and effects of higher budworm populations were both apparent in our satellite imagery. The hardwood component, revealed by a higher NIR in the 1987 scene, was a determining factor for lower budworm population levels in 1993. The green needle fraction in the demixed 1993 imagery detected the effect of higher budworm populations: actual defoliation. This raises the question of what was detected by previous defoliation classifications. High defoliation classification accuracy, or a good correlation between insect populations and satellite data, does not necessarily correspond to actual defoliation.

This is less important for the rapid assessments of current outbreaks. However, separating determining factors versus effects of higher insect population levels is crucial for scientific studies aimed at understanding the spatial dynamics of insect outbreaks.

To our knowledge, this study was the first to use insect population data as calibration data instead of visual defoliation estimates. Visual estimates introduce uncertainty into the analysis and may be part of the reason why previous studies could only derive a few defoliation classes. Populations of defoliating insects are routinely monitored by resource management agencies. Correlating these data sets with satellite data may improve understanding about the determining factors and the effects of insect populations.

The hardwood species component, apparent as higher NIR reflectance in the 1987 imagery, was negatively correlated with 1993 budworm populations. A similar relationship has been found for spruce budworm (Su et al., 1996). More diverse stand species mixture had been suggested as a management tool to reduce future jack pine budworm outbreak levels (Weber, 1995). The life history of jack pine budworm provides a possible ecological reason for this relationship. Budworm populations spread spatially when the female moths disperse. The likelihood of a moth successfully dispersing into a stand is higher when there is a high percentage of jack pine in the surrounding landscape.

CONCLUSIONS

Detecting and forecasting insect defoliation is important both for forest managers and for forest ecologists. Previous studies that used remotely sensed data focused almost exclusively on the detection of defoliation [but see Luther et al. (1997)]. This can be misleading because of the problems involved in separating determining factors and effects of higher insect population levels. Satellite data may be correlated with both forest attributes that limit insect populations (e.g., hardwood content), and actual defoliation. Our analysis of jack pine budworm defoliation showed lower budworm population levels at higher pre-outbreak NIR (due to hardwood content) but increasing NIR due to defoliation. Determining factor and effect had conflicting influences on satellite-measured reflectance. We did not attempt to detect defoliation in mixed jack pine stands, but separated mixed and pure stands. The influence of hardwood overruled the subtle reflectance changes due to defoliation (Ekstrand, 1994).

Spectral mixture analysis provided a tool for the reliable detection of insect defoliation. Budworm population field data and the resulting green vegetation fraction exhibited a high correlation ($r=-0.94$). Tests with various endmember sets always resulted in high correlations when a three-endmember set containing bark, green vegetation, and shade endmembers was used. However, the resulting fractions were variable for different endmember sets. The nonphotosynthetic vegetation (NPV) fraction images cannot be interpreted as the percentage of dead vs. green needles, or the percentage of dead versus living trees.

Whereas previous studies achieved highest accuracy in detecting defoliation using change-detection methods, our approach was most successful when applied to single date imagery recorded at the peak of the outbreak. However, we did not compare the results of the spectral mixture analysis with change detection results based on other image transformation techniques such as principal component analysis, or Tasseled Cap transformation, which would be valuable future research.

J. Hill and P. Hostert (Remote Sensing Department, University of Trier, Germany) provided software and gave most valuable advice for the atmospheric correction and spectral mixture analysis described herein. They also assisted in making the spectrometer measurements of jack pine bark and dry needles in their laboratory. M. Smith provided spectral mixture analysis software and gave important guidance in the initial stages of this project. F. Hall, D. Williams, and C. Walthall generously provided spectrometer measurements taken during the BOREAS project and on the Superior National Forest. R. Endreson and S. Weber (Wisconsin Department of Natural Resources) collected and S. M. Gorham entered the jack pine budworm population data. T. Gower, R. Guries, P. Hostert, T. Lillesand, and P. Pope made valuable comments on earlier versions of this manuscript. J. Franklin and one anonymous reviewer provided a thorough and very helpful review. Our sincere thanks to all of them. This research was funded by the Wisconsin Department of Natural Resources, in part by funds from the Federal Aid in Wildlife Restoration Act, Pitman-Robertson Projects #W-160-P and W-160-R; and by the College of Agricultural and Life Sciences, University of Wisconsin–Madison, McIntire-Stennis Project #3885. This paper is a portion of a Ph.D. dissertation prepared by the first author at the University of Wisconsin–Madison.

REFERENCES

Adams, J. B., Sabol, D. E., Kapos, V., et al. (1995), Classification of multispectral images based on fractions of endmembers: application to land-cover change in the Brazilian Amazon. *Remote Sens. Environ.* 52:137–154.

Ahern, F. J. (1988), The effects of bark beetle stress on the foliar spectral reflectance of lodgepole pine. *Int. J. Remote Sens.* 9:1451–1468.

Ahern, F. J., Erdle, T., Maclean, D. A., and Kneppeck, I. D. (1991), A quantitative relationship between forest growth rates and Thematic Mapper reflectance measurements. *Int. J. Remote Sens.* 12:387–400.

Ashley, M. D., Rea, J., and Wright, L. (1976), Spruce budworm damage evaluation using aerial photography. *Photogramm. Eng. Remote Sens.* 42:1265–1272.

Borel, C. C., and Gerstl, S. A. W. (1994), Nonlinear spectral mixing models for vegetative and soil surfaces. *Remote Sens. Environ.* 47:403–416.

Borgerding, E. A., Bartelt, G. A., and McCown, W. M., Eds. (1995), The future of pine barrens in northwest Wisconsin:

a workshop summary, Wisconsin Department of Natural Resources, Madison.

Buchheim, M. P., Maclean, A. L., and Lillesand, T. M. (1985), Forest cover type mapping and spruce budworm defoliation detection using simulated SPOT imagery, *Photogramm. Eng. Remote Sens.* 51:1115–1122.

Collins, J. B., and Woodcock, C. E. (1994), Change detection using the Gramm–Schmidt transformation applied to mapping forest mortality. *Remote Sens. Environ.* 50:267–279.

Collins, J. B., and Woodcock, C. E. (1996), An assessment of several linear change detection techniques for mapping forest mortality using multitemporal Lansat TM data. *Remote Sens. Environ.* 56:66–77.

Coppin, P. R., and Bauer, M. E. (1994), Processing of multitemporal Landsat TM imagery to optimize extraction of forest cover change features, *IEEE Trans. Geosci. Remote Sens.* 32:918–927.

Coppin, P. R., and Bauer, M. E. (1996), Digital change detection in forest ecosystems with remotely sensed imagery. *Remote Sens. Rev.* 13:207–234.

Cross, A. M., Settle, J. J., Drake, N. A., and Paivinen, R. (1991), Subpixel measurements of tropical forest cover using AVHRR data. *Int. J. Remote Sens.* 12:1119–1129.

Dekker, A. G., and Donze, M. (1994), Imaging spectrometry as a research tool for inland water resources analysis. In *Imaging Spectrometry—A Tool for Environmental Observations* (J. Hill and J. Mégier, Eds.), ECSC, EEC, EAEC, Brussels and Luxembourg, pp. 295–317.

Donchenko, V. V., Goltsova, N. I., Johannessen, O. M., Bobylev, L. P., Pitulko, V. M., and Kritsuk, S. G. (1998), Synergistic use of SAR and other satellite data to monitor damaged areas of boreal forests for St. Petersburg region. In *Proc. 27th Int. Symp. Remote Sens. Environ.*, 8–12 June, Tromsø, Norway. Norwegian Space Center, Oslo, Norway.

Ekstrand, S. (1990), Detection of moderate damage on Norway spruce using Landsat TM and digital stand data. *IEEE Trans. Geosci. Remote Sens.* 28:685–692.

Ekstrand, S. (1994), Assessment of forest damage with Landsat TM: correction for varying forest stand characteristics. *Remote Sens. Environ.* 47:291–302.

Foody, G. M., and Cox, D. P. (1994), Sub-pixel land cover composition estimation using a linear mixture model and fuzzy membership functions. *Int. J. Remote Sens.* 15:619–631.

Foody, G. M., Lucas, R. M., Curran, P. J., and Honzak, M. (1997), Mapping tropical forest fractional cover from coarse spatial resolution remote sensing imagery. *Plant Ecol.* 131: 143–154.

Franklin, S. E. (1989), Classification of hemlock looper defoliation using SPOT HRV imagery. *Can. J. Remote Sens.* 15:178–182.

Franklin, S. E., and Raske, A. G. (1994), Satellite remote sensing of spruce budworm forest defoliation in western Newfoundland. *Can. J. Remote Sens.* 20:37–48.

Franklin, S. E., Waring, R. H., McCreight, R. W., Cohen, W. B., and Fiorella, M. (1995), Aerial and satellite sensor detection and classification of western spruce budworm defoliation in a subalpine forest. *Can. J. Remote Sens.* 21:299–308.

Fung, T., and LeDrew, E. (1987), Application of principal components analysis to change detection. *Photogramm. Eng. Remote Sens.* 53:1649–1658.

Gong, P. (1993), Change detection using principal component analysis and fuzzy set theory. *Can. J. Remote Sens.* 19:22–29.

Green, K., Kempka, D., and Lackey, L. (1994), Using remote sensing to detect and monitor land-cover and land-use change. *Photogramm. Eng. Remote Sens.* 60:331–337.

Hall, F. G., Huemmrich, K. F., Strebel, D. E., Goetz, S. J., Nickeson, J. E., and Woods, K. D. (1992), Biophysical, morphological, canopy optical property, and productivity data from the Superior National Forest, NASA/Goddard Space Flight Center, Greenbelt, MD, 137 pp.

Hall, F. G., Shimabukuro, Y. E., and Huemmrich, K. F. (1995), Remote sensing of forest biophysical structure using mixture decomposition and geometric reflectance models. *Ecol. Appl.* 5:993–1013.

Hall, R. J., Crown, P. H., and Titus, S. J. (1984), Change detection methodology for aspen defoliation with Landsat MSS digital data. *Can. J. Remote Sens.* 10:135–142.

Hall, R. J., Titus, S. J., and Volney, W. J. A. (1993), Estimating top-kill volumes with large-scale photos on trees defoliated by the jack pine budworm. *Can. J. For. Res.* 23:1337–1346.

Häne, T. (1991), Spectral interpretation of changes in forests using satellite scanner images, *Acta For. Fenn.* 222:1–111.

Herrmann, K., Rock, B. N., Ammer, U., and Paley, H. N. (1988), Preliminary assessment of airborne spectrometer and airborne thematic mapper data acquired for forest decline areas in the Federal Republic of Germany. *Remote Sens. Environ.* 24:129–149.

Hill, J. (1993), High precision land cover mapping and inventory with multi-temporal earth observation satellite data, EUR 15271, European Communities, Luxembourg, 90 pp.

Hill, J., Mehl, W. and Radeloff, V. C. (1995): Improved forest mapping by combining corrections of atmospheric and topographic effects in Landsat TM imagery. In *Sensors and Environmental Applications of Remote Sensing* (J. Askne, Ed.), Balkena, Rotterdam, pp. 143–151.

Hopkins, P. F., Maclean, A. L., and Lillesand, T. M. (1988), Assessment of Thematic Mapper imagery for forestry applications under Lake States conditions. *Photogramm. Eng. Remote Sens.* 54:61–68.

Hurcom, S. J., Harrison, A. R., and Taberner, M. (1996), Assessment of biophysical vegetation properties through spectral decomposition techniques. *Remote Sens. Environ.* 56: 203–214.

Johnson, E. A., and Gutsell, S. L. (1993), Heat budget and fire behaviour associated with the opening of serotinous cones in two *Pinus* species. *J. Veg. Sci.* 4:745–750.

Joria, P. E., Ahearn, S. C., and Connor, M. (1991), A comparison of the SPOT and Landsat Thematic Mapper satellite systems for detecting gypsy moth defoliation in Michigan. *Photogramm. Eng. Remote Sens.* 57:1605–1612.

Lambin, E. F., and Strahler, A. H. (1994), Change-vector analysis in multitemporal space: a tool to detect and categorize land-cover change processes using high temporal-resolution satellite data. *Remote Sens. Environ.* 48:231–244.

Leckie, D. G., and Ostaff, D. P. (1988), Classification of airborne Multispectral Scanner data for mapping current defoliation caused by the spruce budworm. *For. Sci.* 34:259–275.

Leckie, D. G., Ostaff, D. P., Teillet, P. M., and Fedosjews, G. (1989), Spectral characteristics of tree components of balsam fir and spruce damaged by spruce budworm. *For. Sci.* 35:582–600.

Leckie, D. G., Yuan, X., Ostaff, D. P., Piene, H., and MacLean, D. A. (1992), Analysis of high resolution multispectral MEIS imagery for spruce budworm damage assessment on a single tree basis. *Remote Sens. Environ.* 40:125–136.

Luther, J. E., Franklin, S. E., Judak, J., and Meades, J. P. (1997), Forecasting the susceptibility and vulnerability of balsam fir stands to insect defoliation with Landsat Thematic Mapper data. *Remote Sens. Environ.* 59:77–91.

Macomber, S. A., and Woodcock, C. E. (1994), Mapping and monitoring conifer mortality using remote sensing in the Lake Tahoe valley. *Remote Sens. Environ.* 50:255–266.

McCullough, D. G., Marshal, L. D., Buss, L. J., and Kouki, J. (1996), Relating jack pine budworm damage to stand inventory variables in northern Michigan. *Can. J. For. Res.* 26:2180–2190.

Muchoney, D. M., and Haack, B. N. (1994), Change detection for monitoring forest defoliation. *Photogramm. Eng. Remote Sens.* 60:1243–1251.

Mukai, Y., Sugimura, T., Watanabe, H., and Wakamori, K. (1987), Extraction of areas infested by pine bark beetle using Landsat MSS data. *Photogramm. Eng. Remote Sens.* 53:77–81.

Nelson, R. F. (1983), Detecting forest canopy change due to insect activity using Landsat MSS. *Photogramm. Eng. Remote Sens.* 49:1303–1314.

Proy, C., Tanré, D., and Deschamps, P. Y. (1989), Evaluation of topographic effects in remotely sensed data. *Remote Sens. Environ.* 30:21–32.

Radeloff, V. C., Hill, J., and Mehl, W. (1997), Forest mapping from space–-enhanced satellite data processing by spectral mixture analysis and topographic corrections, EUR 17702, European Communities, Luxembourg, 90 pp.

Radeloff, V. C., Mladenoff, D. J., Manies, K. L., and Boyce, M. S. (1998), Using historical data to analyze forest landscape restoration potential: pre-settlement and current distribution of oak in the northwest Wisconsin Pine Barrens. *Trans. Wisc. Acad. Sci. Arts Lett.* 86:189–205.

Radeloff, V. C., Mladenoff, D. J., and Boyce, M. S. (in press), Effects of jack pine budworm defoliation and salvage harvesting on landscape patterns. *Ecol. Appl.*

Roberts, D. A. (1993), Green vegetation, nonphotosynthetic vegetation, and soils in AVIRIS data. *Remote Sens. Environ.* 44:255–269.

Rock, B. N., Vogelmann, J. E., Williams, D. L., Vogelmann, A. F., and Hoshizaki, T. (1986), Remote detection of forest damage. *BioScience* 36:439–445.

Royle, D. D., and Lathrop, R. G. (1997), Monitoring hemlock forest health in New Jersey using Landsat TM data and change detection techniques. *For. Sci.* 43:327–335.

Settle, J. J., and Drake, N. A. (1993), Linear mixing and the estimation of ground cover portions. *Int. J. Remote Sens.* 14:1159–1177.

Singh, A. (1989), Digital change detection techniques using remotely sensed data. *Int. J. Remote Sens.* 10:989–1003.

Sirois, J., and Ahern, F. J. (1989), An investigation of SPOT HRV for detecting recent mountain pine beetle mortality. *Can. J. Remote Sens.* 14:104–110.

Smith, M. O., Ustin, S. O., Adams, J. B., and Gillespie, A. R. (1990), Vegetation in deserts. I: A regional measure of abundance from multispectral images. *Remote Sens. Environ.* 31:1–26.

Su, Q., MacLean, D. A., and Needham, T. D. (1996), The influence of hardwood content on balsam fir defoliation by spruce budworm. *Can. J. For. Res.* 26:1620–1628.

Tanré, D., Herman, M., Deschamps, P. Y., and De Leffe, A. (1979), Atmospheric modelling of the background contribution upon space measurements of ground reflectance, including bi-directional properties. *Appl. Opt.* 18:3587–3594.

Tanré, D., Deroo, C., Duhaut, P., et al. (1985), Effects atmosphériques en télédétection, logiciel desimulation du signal satéllitaire dans le spectre solaire. In *Proceedings of the 3rd International Colloquium on Spectral Signatures of Objects in Remote Sensing*, Les Arcs/France, Institut National de la Recherche Agronomique, Paris, France, pp. 315–319.

Tanré, D., Deschamps, P. Y., Duhaut, P., and Herman, M. (1987), Adjacency effect produced by the atmospheric scattering in Thematic Mapper data. *J. Geophys. Res.* 92(D10): 12,000–12,006.

Vogelmann, J. E., and Rock, B. N. (1988), Assessing forest damage in high-elevation coniferous forests in Vermont and New Hampshire using Thematic Mapper data. *Remote Sens. Environ.* 24:227–246.

Vogelmann, J. E., and Rock, B. N. (1989), Use of Thematic Mapper data for the detection of forest damage caused by the Pear Thrips. *Remote Sens. Environ.* 30:217–225.

Weber, S. D. (1995), Integrating budworm into jack pine silviculture in northwest Wisconsin. In *Proceedings of the Jack Pine Budworm Symposium* (W. J. A. Volney, V. G. Nealis, G. M. Howse, A. R. Westwood, D. G. McCullough, and B. L. Laishley, Eds.), Winnipeg, Manitoba, January 24–26 1995, pp. 19–24.

Wessman, C. A., Bateson, C. A., and Benning, T. L. (1997), Detecting fire and grazing patterns in tallgrass prairie using spectral mixture analysis. *Ecol. Appl.* 7:493–511.

Westman, W. E., and Price, C. V. (1988), Detecting air pollution stress in southern California vegetation using Landsat Thematic Mapper band data. *Photogramm. Eng. Remote Sens.* 54:1305–1311.

Williams, D. L. (1991), A comparison of spectral reflectance properties at the needle, branch, and canopy level for selected conifer species. *Remote Sens. Environ.* 35:79–93.

Williams, D. L., and Nelson, R. F. (1986), Use of remotely sensed data for assessing forest stand conditions in the eastern United States. *IEEE Trans. Geosci. Remote Sens.* 24:120–138.

Wolter, P. T., Mladenoff, D. J., Host, G. E., and Crow, T. R. (1995), Improved forest classification in the Northern Lake States using multi-temporal Landsat imagery. *Photogramm. Eng. Remote Sens.* 61:1129–1143.